Complex transformations of chemical signals passing through a passive barrier

J. Sielewiesiuk[1,*] and J. Górecki[1,2,†]
[1]*Institute of Physical Chemistry, Polish Academy of Sciences, Kasprzaka 44/52, 01-224 Warsaw, Poland*
[2]*ICM UW, Pawińskiego 5A, 02-106 Warsaw, Poland*
(Received 27 February 2002; published 23 July 2002)

It has been recently observed that a passive barrier separating two excitable chemical media may transform the frequency of a train of incoming pulses. In this work we apply the FitzHugh-Nagumo-type model to study this phenomenon in a detailed way. Our numerical calculations demonstrate that at the barrier a periodic train of pulses may be transformed into a complex output signal. The ratio of frequencies of the output and the input signals, plotted as a function of the barrier's width or as a function of the input signal frequency, has a devil's-staircase-like shape.

DOI: 10.1103/PhysRevE.66.016212 PACS number(s): 05.45.−a, 89.75.Kd, 82.40.Ck

I. INTRODUCTION

Properties of chemical excitable systems have been studied for many years [1]. These systems are characterized by a single steady state and they answer to perturbations in a very characteristic way. Small-amplitude perturbations are rapidly dumped out, but perturbations with a large amplitude are amplified and the system returns to its steady state after much longer time than in the case of a small perturbation. The evolution forms a closed trajectory (so-called excitation cycle) in the phase space. For a given type of perturbation we can introduce s_{min} as the minimum strength of perturbation that leads to the system's excitation. The excitable systems have another interesting feature: just after an excitation they become refractory with respect to consecutive perturbations and a certain amount of time (refractory time) is needed before they can be reexcited. The refractory time t_r is schematically shown in Fig. 1(a).

Let us consider two successive perturbations, occurring at times 0 and t. Let us fix the strength s of these perturbations. At time 0 every perturbation characterized by s $(s>s_{min})$ excites the system. A successful excitation by the second perturbation depends on the values of t and s. If s is too small, the system is not excited by the second perturbation, nor by the first one. If the perturbation is strong enough, then reexcitation occurs when $t>t_r$. One may also expect that t_r gets smaller when perturbation's strength increases. The arguments given above indicate that areas of successive reexcitation [marked with ''1'' in Fig. 1(a)] should be placed in the parameter space (t,s) as shown in Fig. 1(a).

For a moment let us assume that the state of the system is not significantly changed after an unsuccessful perturbation and the probability of excitation shown in Fig. 1(a) remains valid if a periodic sequence of perturbations is considered. Now t denotes the time from the last perturbation that excited the system. Let us consider a periodic sequence of perturbations at times $kt_p, k \in N$. It is easy to see that if $t_p > t_r(s)$ then each perturbation will excite the system. If $t_r(s)/2 \leqslant t_p < t_r(s)$ then every second of them will excite the system, if $t_r(s)/3 \leqslant t_p < t_r(s)/2$, then every third perturbation will do it and so on. If we plot the firing number f (ie., the ratio between the frequencies of excitations and perturbations) as a function of t_p [Fig. 1(b)], then we obtain a plot similar to devil's staircase [2]. Another staircaselike plot can be obtained if we represent the firing number as a function of s for a fixed t_p [see Fig. 1(c)].

Of course, the ''naive'' model we have just discussed is extremely crude, but it shows that devil's-staircase-like dependence of firing number on the period of perturbations should be widely observed in excitable systems. It is true indeed. Such dependence can be found in a number of papers concerned with periodic perturbations of a homogeneous excitable system which were published by Marek and coworkers [3–6]. Another staircaselike dependence of the firing number was observed by Toth, Gaspar, and Showalter in spatially distributed excitable systems linked with a capillary tube [7]. The excitable waves were generated in one system and they might excite the other one via reagents' transport in the capillary. In this experiment the diameter of the capillary controlled the strength of perturbation. If it was small, the refractory time of the perturbed system was much longer than the refractory time in the system where waves were originally generated. As a result only a fraction of generated waves excited the system after passing through the capillary and the firing number as the function of entering wave period has a devil's-staircase-like dependence (cf. Fig. 6 in Ref. [7]).

In this paper we are concerned with yet another example of a spatially distributed excitable system, in which such a resonant transformation of excitation occurs.

Let us consider a simple one-dimensional structure, composed of two intervals, in which the system is in an excitable state, separated by a narrow passive barrier, where the time evolution is given by the diffusion equation. Such a system can be seen as a prototype of a plane excitable medium—for example, a membrane filled with an immobilized catalyst, which is divided into two subplanes by a stripe without the catalyst [8]. Within the active areas pulses of excitation may be generated and they can propagate. In the passive barrier reactions do not occur and some of the reagents can just diffuse through it. If we consider pulses of excitation characterized by wave vectors perpendicular to the barrier then

*Email address: kubas@ichf.edu.pl
†Email address: gorecki@ichf.edu.pl

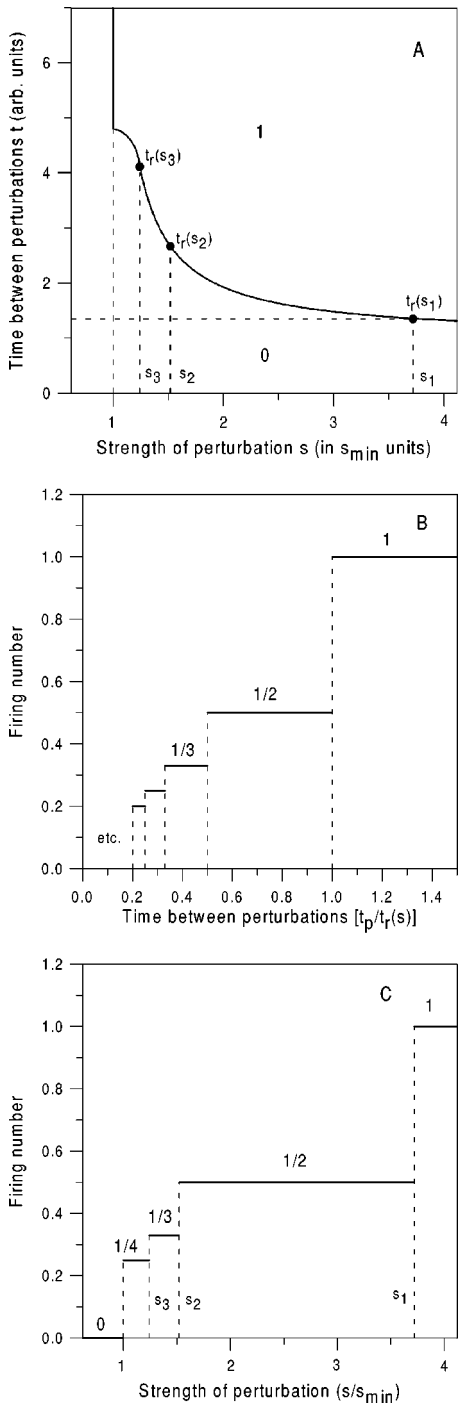

FIG. 1. The ''naive'' model of a perturbed excitable system. Figure 1(a): The probability that the second perturbation excites the system as a function of the strength of perturbation (s) in s_{min} units and the time separating perturbations t. For a given s the line separating the excited systems by the second perturbation from unexcited ones shows $t_r(s)$. Note that for times $t<t_r$ and for $s<1$ the system cannot be excited. Figure 1(b): The firing number as the function of the time interval between consecutive perturbations of the system [in $t_p/t_r(s)$ units] for a fixed strength of perturbation. Figure 1(c): The firing number as the function of the strength of perturbation s, for a fixed t_p.

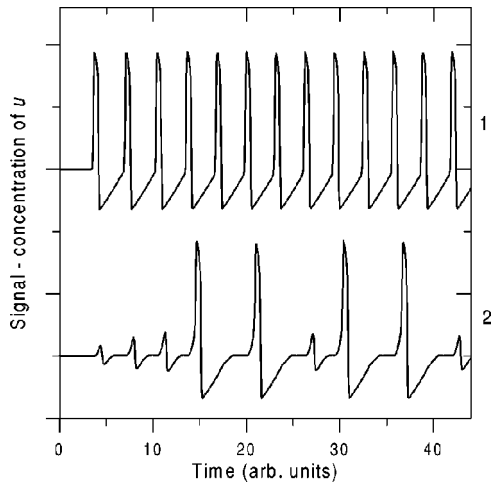

FIG. 2. The time evolution of the value of u before the barrier (curve 1) and just behind it (curve 2). The small maxima (on curve 2) do not develop into regular pulses, so the firing number equals 2/5. We have used the FH-N model with $t_p=3.14$ ($f_p=0.318$), $d=0.1707$, and a uniform grid with $n=251$.

the symmetry allows one to describe the system as one dimensional. We have studied the time evolution of such systems [9] and we have shown that under certain conditions the barrier works as a transformer of the frequency for a regular train of pulses approaching it. As Fig. 2 shows, after a short transient period a stable periodic output signal is observed for the whole time within which the computations are performed ($t_{max}=10\,000$). For the considered frequency of the input signal and barrier's width two out of each five arriving pulses are transmitted, thus the firing number equals 2/5. The transformation of frequency on the barrier was observed for both FitzHugh-Nagumo [10] and Rovinsky-Zhabotinsky models [11–13] of the Belousov-Zhabotinsky reaction [14]. The implications of the frequency transforming by a passive barrier on selected signal processing devices were discussed in Ref. [15]. In our previous papers [9,15] we were mainly concerned with quite simple signal transforming on a barrier, like the division of the original frequency by 2 or 3, because such types of behavior are quite ''robust,'' i.e., they may be observed for a wide range of input signal frequencies and barrier's widths. However, for certain sets of parameters we have also found a more complex output signal. Here we give more information on the frequency transforming phenomenon. The FitzHugh-Nagumo-type model is used for numerical studies. We present new modes of transformation, which were not described in our previous papers. Some of these modes have a high level of complexity. We also discuss the computational difficulties connected with the numerical studies of waves propagating through a passive barrier.

The paper is organized as follows. Section II contains a short description of the FitzHugh-Nagumo model, the numerical method and an overview of the results concerning the frequency transforming on a passive barrier. In Sec. III we indicate the numerical problems we have faced. The new results are presented in Sec. IV. Section V contains the conclusions.

II. TRANSFORMATION OF FREQUENCY ON A PASSIVE BARRIER

A. The FitzHugh-Nagumo model

The FitzHugh-Nagumo (FH-N) model was originally introduced to describe the excitable behavior of nerve tissues [16,17]. It uses two variables (u, v) and the dynamics of the first of them is given by a third-order polynomial in u, whereas the dynamics related to v is a linear function in u and v. Even such a simple model shows an interesting nonlinear behavior. In even more simplified version of FitzHugh-Nagumo model we use, the dynamics in active areas is described by the following equations [10,16,17]:

$$\tau\frac{\partial u}{\partial t} = -\gamma[ku(u-\alpha)(u-1)+v]+D_u\nabla^2 u, \qquad (1)$$

$$\frac{\partial v}{\partial t} = \gamma u \qquad (2)$$

with the parameters $\tau=0.03, \gamma=1, k=3.0, \alpha=0.02$ (as given by Motoike and Yoshikawa in [10]) and $D_u=0.000\,45$ [18]. For these values of parameters the system has a single stationary solution $(u,v)=(0,0)$, homogeneous in space, which is excitable. This system may be excited by a local decrease in the value of v, which initiates a propagating pulse of concentration. The variables u and v cannot be directly associated with concentrations of chemical spices, but their behavior resembles the one of the activator (u) and inhibitor (v) in a chemical system.

We assume that in the passive areas the kinetic terms are absent in the corresponding equations. The diffusion of activator is possible, thus it is natural to call these regions ''diffusion areas.'' The equations describing the time evolution of u and v in these areas are [10]

$$\tau\frac{\partial u}{\partial t} = D_u\nabla^2 u, \qquad (3)$$

$$\frac{\partial v}{\partial t} = 0 = \text{const} \qquad (4)$$

with $\tau=0.03$ and $D_u=0.000\,45$, as in the excitable areas.

B. Numerical integration of reaction-diffusion equations

In this paper we investigate a signal of a high frequency, which passes through a passive barrier. By the signal we understand a regular, stable train of traveling pulses initiated at one end of the system with the frequency f_p. The time evolution of the signal is studied by numerical integration of the reaction-diffusion equations in the active areas and within the barrier [Eqs. (1)–(4)]. For a signal formed by planar waves with the wave vectors perpendicular to the barrier the system can be modeled as an interval of the length l. For numerical integration it is divided into n parts by $n+1$ points of a grid, including both ends (Fig. 3). The distances between the grid points dl may be different; by selecting a fine grid around the barrier we can increase the accuracy of calculations, while a crude grid far away from the barrier saves computer time without affecting the accuracy. In Fig. 3 the black lines correspond to excitable medium and the barrier, indicated by the gray line, is located between grid points n_1 and n_2 $(1 \ll n_1 < n_2 \ll n)$. It means that the evolution of the system at all grid points $j \in [0,n_1] \cup [n_2,n]$ is given by the set of reaction-diffusion equations corresponding to the excitable system [Eqs. (1) and (2)], and the equations describing the passive medium [Eqs. (3) and (4)] give the evolution at all grid points $i \in (n_1, n_2)$. The barrier's width d is estimated as

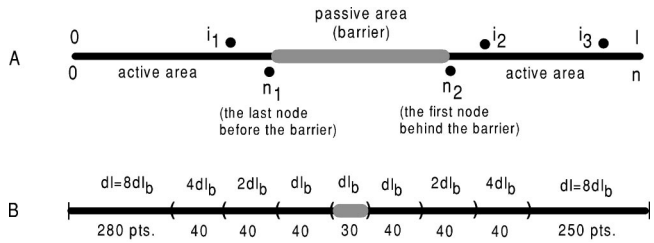

FIG. 3. The scheme of the system studied. Black intervals correspond to active areas, gray ones mark the barrier. Line *A*: the barrier is located between the grid points n_1 and n_2 (excluding n_1, and n_2). The value of u is observed at the grid points i_1, i_2, and i_3. Line *B*: the scheme of the adaptive grid for $n=800$; the distance between grid points is given above the line, the number of grid points separated by a particular dl is given below the line.

$$d \cong (n_2-n_1-1)dl_b, \qquad (5)$$

where dl_b is the distance between neighboring grid points (in our calculations dl_b is constant within the barrier and around it).

There are free flow boundary conditions between passive and active media and no flux boundary conditions at both ends of the interval. Initially both active and passive areas are in their stationary states. Pulses of excitation are initiated at the left end of the interval by a local decrease in the value of v to $v_{ini}=-0.8$ and they travel to the right, coming across the passive barrier on their way. We focus our attention on trains of pulses which are initiated regularly at times kt_p, for selected $t_p>0$ and $k=1,2,3,\ldots,k_{max}$. In the following we distinguish the ''input signal'' (a train of pulses arriving at the barrier) and the ''output signal''—a train of pulses going away after crossing the barrier. The frequency of the input signal is defined as $f_p=1/t_p$.

The concentrations of reagents of interest are calculated using an implicit method based on the Crank-Nicolson discretization of the Laplace operator [19]. The distance between neighboring grid points (dl) is the space step of numerical integration. In our computations we have applied two types of the space grids. In a part of calculations the whole interval l has been divided into n equal parts (in this case $dl=l/n$). We have used equally spaced (uniform) grids with $n=400$, 800 or 1600. The passive gap has been located between $n_1=180$ and $n_2=189$ for $n=400$, $n_1=360$ and $n_2=377$ for $n=800$, and $n_1=720$ and $n_2=753$ for $n=1600$.

In the other calculations we have used adaptive grids, for which the passive barrier and its neighborhood (so the part of the system which has the most important influence on sig-

nal's transformation) has been covered with a fine grid and at both ends of the interval a longer distance between grid points has been used. We have considered a grid formed by $n=800$ grid points and 30 of them are placed within the barrier (the barrier is located between $n_1=400$ and $n_2=431$). The time evolution in the active areas surrounding the barrier has been also calculated using the same fine grid as for the barrier $dl_b=dl/8$. We have considered 40 grid points on each side of the barrier, for which the distance between them is dl_b. Next there are 40 grid points on each side with the distance $2dl_b$ and yet another 40 points with the distance $4dl_b$. The reaction-diffusion equations in the remaining part of the system are solved with a crude grid of dl (see Fig. 3). In order to test the numerical stability we have also used another adaptive grid, for which the total number of grid points is $n=870$ and in this case the passive barrier, located between $n_1=420$ and $n_2=481$, is covered with 60 points of $dl_b=dl/16$. In the active areas located on both sides of the barrier the grid is fine (dl/16,40 points) and next it increases. as follows: dl/8,20 points, dl/4,40 points, and dl/2,40 points. The rest of the system is covered with the space step dl.

The values of activator and inhibitor are recorded at indicators located at the grid points i_1 (before the barrier), i_2 (just behind the barrier), and i_3, far behind the barrier, as shown in Fig. 3. By comparing the time evolutions at i_1, i_2, and i_3 we can tell whether a pulse that arrives at the barrier is able to cross it. Moreover, by counting the number of maxima of activator within a certain time interval we can measure the frequency of the input and the output signals (f_p and f_o, respectively). When calculating f_p and f_o we neglect a few initial pulses (usually 10 or 20) in order to eliminate transient behavior at the beginning of evolution. To describe quantitatively the passive barrier as a device that transforms chemical signal frequency, we introduce the filtering ratio (or a firing number, if notation of Refs. [3–7] is used) defined as f_o/f_p.

C. The frequency transforming on a passive barrier

Let us consider the system shown in Fig. 3. A single pulse of excitation traveling in the excitable medium towards the barrier may cross it, provided that the barrier is narrow enough. It means that the pulse arriving at one side of it excites the active area on the other side and in this case the barrier is transparent to the pulse. The maximum width of a transparent barrier is called the penetration depth d_{max}. Barriers wider than d_{max} are impenetrable for a single pulse, because for a wide barrier the value of diffusing activator at the other end of the barrier is too small to excite the active area behind the barrier. We have found [9,18] that for the parameters of the model used in this study $d_{max}\approx 0.163$.

Now let us consider a train of incoming pulses with a constant frequency f_p. It turns out [9,15] that for a certain range of f_p and barrier's width d the passive gap transforms the frequency of the input signal. It means that the frequency of the transmitted signal f_o (observed behind the barrier) is a fraction of f_p. Some of the incoming pulses are stopped at the barrier, while the others get through.

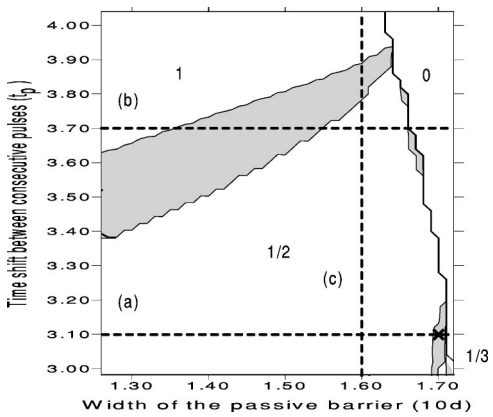

FIG. 4. Filtering ratio (f_o/f_p) for the FitzHugh-Nagumo model as a function of the barrier's width (d) and the time shift between consecutive pulses (t_p). The white, labeled areas correspond to the situation when f_o is the fraction of f_p given in the picture. Gray color marks more complicated transformations of frequency. The dashed lines in Fig. 4 correspond to $(a)t_p=3.10$ ($f_p=0.323$),$(b)t_p=3.70$ ($f_p=0.270$),$(c)d=0.160$. The cross stands for $t_p=3.10$ ($f_p=0.323$) and $d=0.1702$.

Figure 4 presents a diagram in the space of parameters (d,t_p) showing "phases" in which the filtering ratio is some proper fraction given in the diagram (the white regions with labels). For example, in the area labeled as "1" every incident pulse is able to get through the passive barrier (the barrier is transparent to all pulses) and in the area labeled as "1/2" every second of the incident pulses is transmitted. The gray regions between the labeled areas in Fig. 4 correspond to more complex transmission patterns. When d increases we observe that the filtering ratio decreases, which means that the pulses are less and less frequently transmitted. Finally the barrier becomes too wide and no pulse can cross it, which corresponds to the area labeled as "0." The dashed lines in Fig. 4 mark $t_p=3.10(f_p=0.323)$, line (a); $t_p=3.70(f_p=0.270)$, line (b); and $d=0.160$, line (c). The cross stands for $t_p=3.10$ and $d=0.1702$ and shows the parameters used to calculate the time series presented in Fig. 5. The filtering ratios as functions of parameters from the dashed lines $(a),(b)$, and (c) are discussed in Secs. III and IV. Figure 4 has been obtained for a uniform grid with $n=251$ and $dt=5\times10^{-3}$.

Figure 5 illustrates the filtering ratio equal to 1/3 (the region corresponding to 1/3 is located in the bottom right-hand side corner of the diagram in Fig. 4). The values of activator at the grid points: i_1 [the upper curve (1)], i_2 (curve 2), and i_3 (curve 3) (cf. Fig. 3, line A) are presented as a function of time. Curve 1 corresponds to the incident pulses (input signal) with frequency $f_p=0.323$. Curve 2 shows the transmitted pulses (output signal), recorded just behind the barrier. Its frequency $f_o=f_p/3$. It is clear that every third of the incident pulses is able to cross the passive gap. Small oscillations that can be seen on the curve 2 do not develop into pulses and they disappear when the output signal is observed at larger distances behind the barrier (cf. curve 3). The width of the barrier is $d=0.1702$. Figure 5 has been obtained for a uniform grid with $n=400$, $i_1=170$, $i_2=199$, $i_3=390$, and $dt=1\times10^{-3}$.

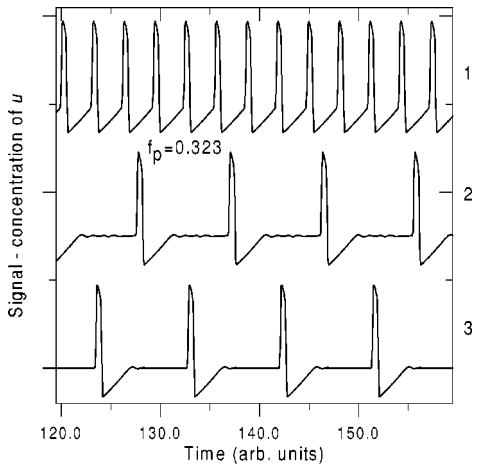

FIG. 5. The time evolution of the value of u at the grid point i_1 (the upper curve 1), at the grid point i_2 (curve 2), and at the grid point i_3 (curve 3). The evolution at i_3 (curve 3) is presented to show that the small maxima appearing on curve 2 disappear at longer distances from the barrier. Filtering ratio equal to 1/3 is illustrated. We have used $t_p=3.10$ ($f_p=0.323$) and $d=0.1702$ (this point is marked with a cross in Fig. 4).

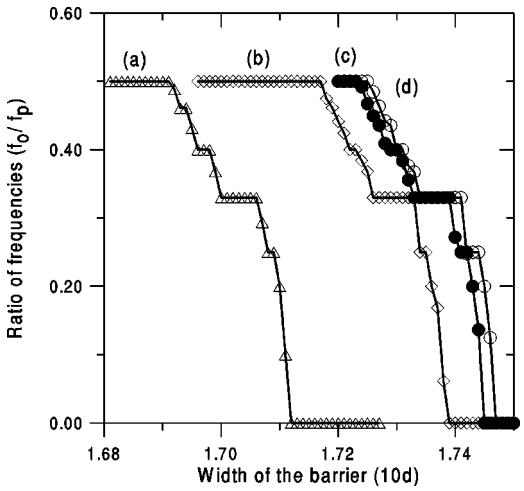

FIG. 6. Filtering ratio f_o/f_p for fixed $t_p=3.10$ ($f_p=0.323$) and d changing within the presented range. All results have been obtained for $dt=1\times10^{-3}$, $t_{max}=500$, but for each of the curves (a)–(d) different grids have been used. This figure illustrates the dependence of the results on computational parameters. Curve (a): marked with empty triangles. ordinary grid with $n=400$. Curve (b): marked with empty diamonds, ordinary grid with $n=800$. Curve (c): marked with filled circles, adaptive grid with $n=800$. Curve (d): marked with empty circles, adaptive grid with $n=870$.

III. NUMERICAL DIFFICULTIES

The solutions that correspond to the filtering ratio 1/2 or 1/3 are quite stable numerically and they cover a large part of the parameters' space. In order to learn more about what happens in the gray areas of Fig. 4 we have performed a series of calculations with one of the parameters (the width of the passive barrier d or the time shift between consecutive incident pulses t_p) fixed and the other changing within a certain range. By monitoring the input and output signals (similar to those presented in Fig. 5) we have been able to calculate the filtering ratio for the given combination of d and t_p and describe the sequence of transmitted/stopped pulses in the input signal, which leads to a particular value of f_o/f_p. The calculations have been done for parameters on the lines of constant d or t_p shown in Fig. 4. The computations have had to be performed for a period of time long enough to observe many full cycles of signal transformation. However, we have discovered that the results of calculations are quite sensitive with respect to the size of the grid and the time integration step (dt) used in computations.

Figure 6 presents a set of curves showing the filtering ratio for $t_p=3.10$ ($f_p=0.323$) as a function of d. The considered values of parameters are situated on the horizontal dashed line (a) in Fig. 4. All results have been obtained for $dt=1\times10^{-3}$ and the calculations have been performed up to $t_{max}=500$. For curve (a) in Fig. 6, marked with empty triangles, a uniform grid with $n=400$ has been used. Curve (b), marked with empty diamonds, indicates the results for a uniform grid with $n=800$. In case of curves (c) (filled circles) and (d) (empty circles) we have used adaptive grids with $n=800$ (c) and $n=870$ (d), respectively. The value of dl_b in these simulations depends on system's length l and the number of grid points used. We have analyzed signals at indicators i_1 and i_2, located at approximately constant distance of $l_i=0.6$ (in the dimensionless units of distance) before and behind the passive gap (cf. Fig. 3, line A).

Results presented in Fig. 6 show a rich structure of different filtering ratios, which is much more complex than the one shown in Fig. 1(c) for the ''naive'' model of an excitable system. Of course, we can observe some similarities: the region of d for which $f_o/f_p=1/2$ is the dominant one, and the second most important is $f_o/f_p=1/3$. But we also see filtering ratios between 1/3 and 1/2, which are absent in the ''naive'' model. The calculations show that although f_o/f_p as a function of d looks very similar for different values of parameters of integration, it shifts towards larger values of d when more accurate integration techniques are applied. A significant shift between curves (a) and (b) in Fig. 6 indicates that for the uniform grids that we have used the results depend on the grid size. It is worth noticing that the behavior of the filtering ratio as a function of d does not change, but the function as a whole is just shifted towards wider barriers. It is expected that for yet finer grid we should obtain results that are numerically stable, but a finer grid means that more grid points should be used to describe a system of the same size. However, in the implicit method of solving parabolic reaction-diffusion equations the solution at each time step is obtained via iterations. In our case the roundup errors have led to instabilities when few thousands of grid points have been used. The adaptive grids (Fig. 3, line B) allow one to obtain more accurate numerical solutions. For such grids the fine resolution within the most important area of the investigated system may be achieved without using large number of grid points, which provides both accuracy and stability of computations. As already mentioned, curve (c) in Fig. 4 has been obtained for the adaptive grid with $n=800$. The resolution in the neighborhood of the passive gap for this grid is

$dl_b = dl/8 \approx 0.06$ (for $l \approx 25.72$), which is four times smaller than dl for the finest uniform grid. For curve (d) this resolution is twice higher, but f_o/f_p as a function of d obtained for both grids [curves (c) and (d)] are almost identical. Therefore we believe that the adaptive grid with $n=800$ grid points is sufficient for our calculations and we have used it to obtain results given below.

Several values of the time step for the integration ($dt = 5\times10^{-3}$, 1×10^{-3}, and 1×10^{-4}) have been used to verify the consistency of the results.Although the implicit algorithms should be in general stable for all values of time and space integration steps, we have observed that numerical instabilities may appear for $dt=5\times10^{-3}$ and large n. On the other hand, the results for $dt=1\times10^{-3}$ and $dt=1\times10^{-4}$ have been regular and consistent. Consequently, we have decided to use $dt=1\times10^{-3}$ for most of calculations described in this study.

IV. COMPLEX PATTERNS OF OUTPUT SIGNALS

The results presented in this section have been obtained for the adaptive grid with $n=800$. The passive area has been located between $n_1=400$ and $n_2=431$ (30 grid points inside the passive barrier). The incoming and outgoing pulses have been monitored at grid points $i_1=390$ and $i_2=441$, respectively. The computations have been carried out with time step $dt=1\times10^{-3}$, up to $t_{max}=500$, if not explicitly stated otherwise. About 150 pulses arrive at the barrier within the selected time t_{max}.

Let us introduce a notation that describes output signal. The incident pulses, observed at i_1 provide a natural time scale in the system. We write "1" if the pulse gets successfully through the passive barrier and is observed at i_2 or "0" otherwise. Thus the output signal may be coded as a sequence of "0" and "1." In such notation a common case in which every second pulse passes (filtering ratio $f_o/f_p = 1/2$) is coded as (01) and the mode "1/3," presented in Fig. 5, is described as (001). It is understood that the given sequence repeats periodically. A pattern coded as $(abc\ldots)^p(def\ldots)^q$ (where p and q are positive integer numbers) means that behind the barrier first the sequence $(abc\ldots)$ is observed p times and next the sequence $(def\ldots)$ appears q times. In this notation, nonperiodic modes correspond to an infinite sequence of $(abcde\ldots)$. If pattern's sequence is finite then it is very easy to calculate the corresponding filtering ratio f_o/f_p because it equals to the sum of the symbols in the sequence divided by the number of symbols. For nonperiodic modes we can estimate the filtering ratio using a finite part of the sequence and of course the more pulses are taken into account, the better approximation is achieved.

Figure 7 presents the filtering ratio for $t_p=3.10(f_p = 0.323)$ as a function of the width of the passive barrier changing from 0.171 to 0.176 with increment of 0.0001 (this has been achieved by changing the total length of the system l from 27.49 to 28.19 with increment of 0.016). This value of t_p corresponds to line (a) in Fig. 4. The results coming from our computations are marked with filled circles. In Fig. 7 one may notice several plateaus, which correspond to simple patterns of frequency transforming and are labeled with appropriate filtering ratios. Looking from left to the right we have modes: "1/2" with the sequence (01),"2/5" with (01)$\times$(001),"1/3" with (001),"1/4" with (0001), and finally "0" with the sequence 0. It is remarkable that a "simple" frequency transformation occurs within a wider range of barrier's width than a complex one. Other interesting transmission patterns, located between those plateaus, have also been observed, but the ranges of values of d, within which those patterns appear, are so narrow that we have detected them just for a single width of the barrier. The unique patterns have been labeled with letters a–k in Fig. 7. Probably the most complicated transmission pattern is associated with point a, located just below the plateau "1/2." In this case the sequence of pulses behind the barrier is $(01)^{14}(001)\times(01)^{13}(001)$ and the corresponding filtering ratio $f_o/f_p = 29/60$. For point b in Fig. 7 the corresponding pattern is $(01)^4(001)(01)^5(001)$ resulting in $f_o/f_p=11/24$, for point c it is $(01)^3(001), f_o/f_p=4/9$; for point d it is $(01)^2(001)$, $f_o/f_p=3/7$; for point e it is $(01001)^3(0101001), f_o/f_p = 9/22$; for point f it is $(01)(001)^2, f_o/f_p=3/8$; for point g it is $(01)(001)^6, f_o/f_p=7/20$; for point h it is $(001)\times(0001), f_o/f_p=2/7$; for point j it is $(00001), f_o/f_p=1/5$, and point k it is $(0000001), f_o/f_p=1/7$.

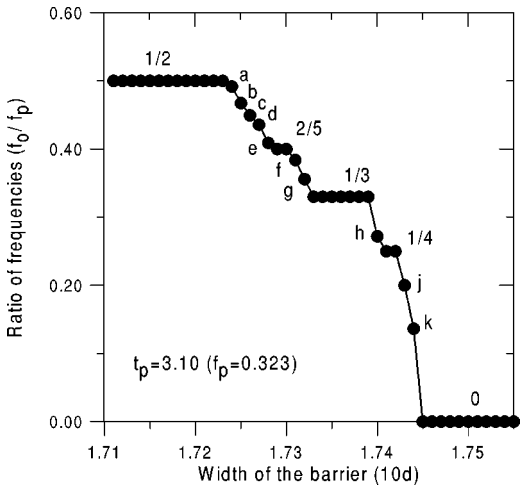

FIG. 7. Filtering ratio f_o/f_p for fixed $t_p=3.10$ ($f_p=0.323$) and d changing within the presented range. The filled circles correspond to computational points. The curve forms several plateaus that are labeled with corresponding values of the filtering ratio (1/2, 2/5, 1/3, 1/4, and 0). At points labeled a–k other values of f_o/f_p (and other transmission patterns) have been observed. These values as well as all the sequences of transmitted pulses are given in text (Sec. IV).

Figure 4 suggests that transmission patterns corresponding to filtering ratios greater than 1/2 are also present. Such patterns are absent in the "naive" model of excitable systems [Figs. 1(b) and (c)]. To see them clearly calculations for $t_p = 3.70(f_p=0.270)$ have been performed for the barrier's width d changing from 0.130 to 0.171 with increment of 0.001 (l changing from 20.93 to 27.49 with increment of 0.16). This value of t_p corresponds to line (b) in Fig. 4. The results are plotted in Fig. 8. Indeed, one may see here several plateaus, labeled with corresponding filtering ratios, which

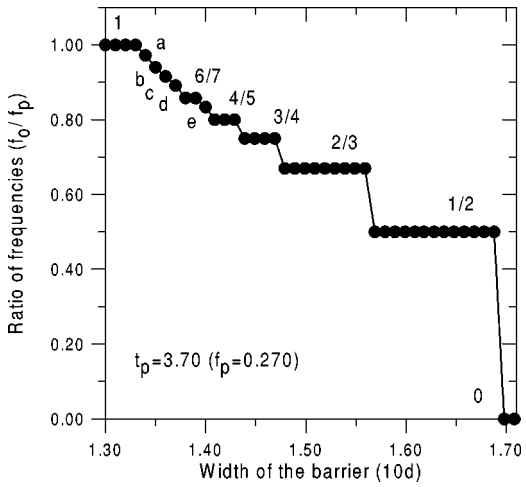

FIG. 8. Filtering ratio f_o/f_p for fixed $t_p=3.70$ ($f_p=0.270$) and d changing within the presented range. The filled circles correspond to computational points. The plateaus are labeled with corresponding values of the filtering ratio (1, 6/7, 4/5, 3/4, 2/3, 1/2, and 0). At points labeled a–e other values of f_o/f_p (and other transmission patterns) have been observed. These values as well as all the sequences of transmitted pulses are given in text (Sec. IV).

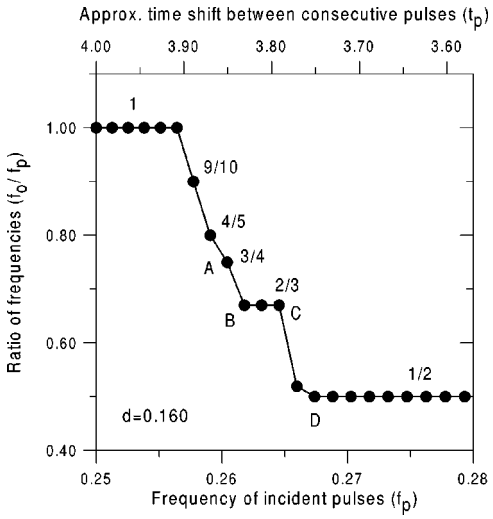

FIG. 9. Filtering ratio f_o/f_p for fixed $d=0.160$ and f_p changing from 0.25 to 0.28 (see the bottom axis), which corresponds to t_p decreasing from 4.00 to 3.57 (see the approximate top axis). The filled circles correspond to computational points. The plateaus as well as single points are labeled with corresponding values of f_o/f_p (1, 9/10, 4/5, 3/4, 2/3, and 1/2). The letters A,B,C, and D mark the intervals of the diagram which have been studied with a higher resolution. The results for the interval A-B are presented in Fig. 10(a) and for the interval C-D in Fig. 10(b).

are greater than 1/2. From left to right we have: plateau "1" with the sequence (1); plateau "6/7" with (0111111); plateau "4/5" with (01111); plateau "3/4"with (0111); plateau "2/3" with (011); plateau "1/2" with (01), and plateau "0" with the trivial transmission pattern (0). Moreover, we have observed more complex output signals. The points labeled by letters correspond to the following patterns and filtering ratios: point a, $(0)(1)^{35}, f_o/f_p=35/36$; point b, $(0)(1)^{14}, f_o/f_p=14/15$; point c, $(0)(1)^{10}, f_o/f_p=10/11$; point d, $(0)(1)^{8}, f_o/f_p=8/9$, and point e $(011111), f_o/f_p=5/6$. The output signals observed here are dual to those with filtering ratios smaller than 1/2.

Figure 9 presents the filtering ratio for $d=0.160$ ($l=25.72$) plotted versus the frequency of incident pulses $f_p\in[0.25,0.28]$ (the time shift between consecutive pulses changing from 3.57 to 4.00 with increment of 0.02; approximate values of t_p are given on the top axis of Fig. 9). These values of d are placed on the line (c) in Fig. 4. The numerical labels in Fig. 9 give the filtering ratio observed for corresponding plateaus or points. Looking at Fig. 9 from left to the right we have: plateau "1" with the sequence (1); point "9/10" with the sequence $(0)(1)^9$; point "4/5" with (01111); point "3/4" with (0111); plateau "2/3" with (011) and plateau "1/2" with (01). In order to check if the filtering ratio is a monotonic function of f_p we have performed a number of calculations for $f_p\in[0.2604,0.2618]$ and for $f_p\in[0.2646,0.2674]$. The ends of these intervals correspond to f_p for points A,B,C, and D in Fig. 9. We have probed the system's behavior using $\delta t_p=0.002$ (corresponding to $\delta f_p=0.000\,14$). In the interval A-B the behavior is trivial, which means that the studied systems splits into two classes corresponding to (0111) and (011) modes [see Fig. 10(a)].

Similar calculations have been performed for systems located between points C and D in Fig. 9 (it corresponds to $f_p\in[0.2646,0.2674]$). In this case we have observed two patterns [α and β, see Fig. 10(b)] between the plateaus corresponding to filtering ratios 2/3 [(011) mode] and 1/2 [(01) mode]. One of these patterns (β) describes quite simple transformation of the original signal to (01)(011) mode, which is just 1:1 mixture of the neighboring modes. The other point (α) corresponds to a more interesting behavior. Using the same dt and dl_b as for the other points shown in Fig. 10(b) (filled circles) we have observed $f_o/f_p=0.519\,17$. The decrease in time step dt increases the filtering ratio as follows: $dt=1\times10^{-4}$ gives $f_o/f_p=0.556\,02$ (empty circle), $dt=2\times10^{-5}$ gives $f_o/f_p=0.575\,94$ (empty triangle), and $dt=1\times10^{-5}$ gives $f_o/f_p=0.578\,95$ (cross). Moreover, we have observed that times between transmitted pulses are not always a multiplicity of t_p. In order to explain it we have examined the time evolution $u(t)$ at the points i_1 and i_2. Figure 11 shows the relevant part of it. One can notice that in some cases the transmitted signal does not develop into a pulse, $u(t)$ slightly decreases and then it starts to increase again, forming a pulse shifted with respect to the forcing signal. Such a strange behavior for $f_p=0.2660(t_p=3.76)$ does not disappear when we decrease dt and dl_b. The moment it appears first and the time intervals between successive strange excitations depend on dt, but we do not observe any regularities. The presence of irregular "strange excitations" makes the filtering ratio at the point α dependent on dt. f_o/f_p at this point still remains smaller than 0.6 so we cannot exclude a nonmonotonic dependence of the filtering ratio on f_o/f_p. Moreover, such strange excitations are observed for the whole range of time steps we have used, so we are unable to blame numerical instabilities for their presence. The time evolution of the output signal between the strange

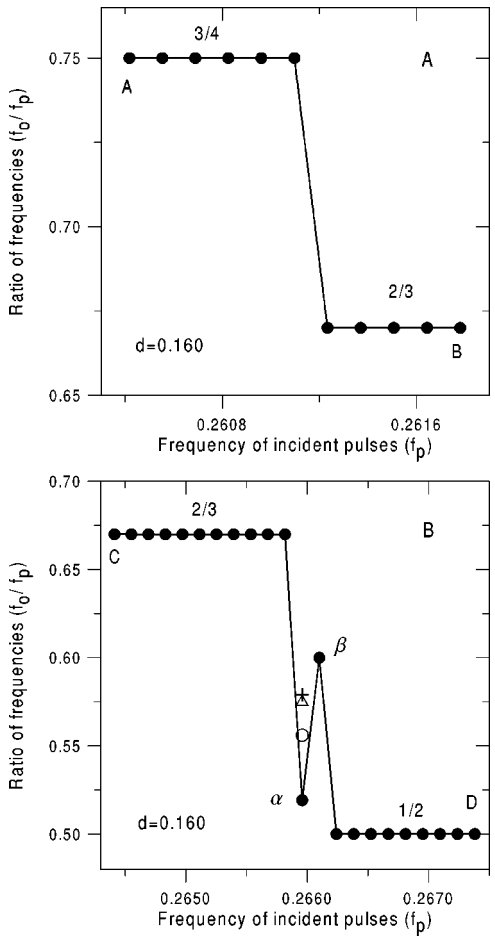

FIG. 10. Results of a more detailed examination of intervals *A*-*B* and *C*-*D* from Fig. 9. Figure 10(a): Filtering ratio f_o/f_p for fixed $d=0.160$ and f_p changing from 0.2604 to 0.2618. Points *A* and *B* in this figure correspond exactly to points *A* and *B* in Fig. 9. We do not observe any filtering ratios different from 3/4 or 2/3. Figure 10(b): Filtering ratio f_o/f_p for fixed $d=0.160$ and f_p changing from 0.2646 to 0.2674. The filled circles mark the computational points. Points *C* and *D* in this figure correspond exactly to points *C* and *D* in Fig. 9. We have found a ''strange'' point α between plateaus 2/3 and 1/2 (labeled with values of the filtering ratio), for which the value of f_o/f_p depends on the time step of integration. Different symbols mark the values of the filtering ratio obtained for: $dt=1\times10^{-3}$ (filled circle), $dt=1\times10^{-4}$ (empty circle), $dt=2\times10^{-5}$ (empty triangle), $dt=1\times10^{-5}$ (cross). In the studied region we have observed the point β, that is regular and corresponds to the transmission pattern (01)(011) (thus $f_o/f_p=3/5$).

excitations is a mixture of (01) and (011) modes with different proportions.

V. CONCLUSIONS

In this study we are concerned with the signals obtained after a regular train of pulses crosses a barrier of a passive medium. The calculations have been performed for the excitable medium described by the FH-N model, but we believe that qualitatively the results may be applied to any excitable system.

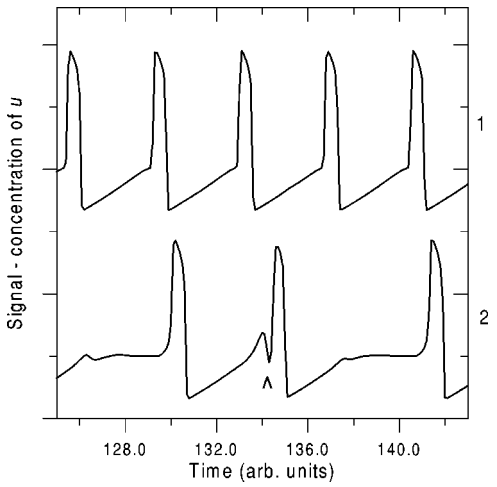

FIG. 11. A part of the time evolution of the value of *u* at the grid point i_1 (input signal is represented by the upper curve 1) and at the grid point i_2 (output signal is represented by curve 2) observed for $d=0.160, f_p=0.2660$ with $dt=1\times10^{-5}$ [point α is represented by the cross in Fig. 10(b)]. The arrow marks the position of the strange excitation in the output signal.

We have observed many different patterns of the transmitted signal, which depend on the frequency of the input signal on the barrier's width. We have found that the mode in which every second pulse from the input signal is transmitted [(01) mode] is the most common one for which a nontrivial transformation [i.e., different from (0) or (1)] of the original signal occurs and it is observed for a wide range of parameters. We have also found a family of transmitted signals in which one signal out of *n* arriving gets through the barrier [$(0)^{n-1}(1)$ mode]. These signals, characterized by the firing number $1/n$, contribute to the devil's-staircase-like behavior of the firing number, expected on the basis of the ''naive'' model of a perturbed excitable system. However, we have also observed less trivial patterns of the transmitted signal. There is another interesting family of transmitted signals, which can be described as $(0)(1)^{n-1}$ and corresponds to the case when only one signal is not transmitted out of every *n* arriving. Such behavior cannot be described by the ''naive'' model, but comes out quite naturally, if one assumes that an excitable system that has not reached the stationary state may be reexcited by a perturbation that is strong enough (see discussion in Ref. [7]). Finally, we have observed many complex structures of the output signal, which follow the structure of the Farey tree [20] (take, for example, points a–h in Fig. 7).

In the paper we have focused a lot of attention on the numerical aspects of the problem, because the very complex patterns that we observed were related to the numerical instabilities and disappeared when more accurate numerical integration methods were applied [with the sole exception of the point α—Fig. 10(b)—for which evolution was complex for any method of numerical integration].

Finally, we would like to mention that structured signals have a transient character. It is known that the velocity of a pulse of excitation increases when its distance to the

previous pulse is larger [21]. Thus, far behind the barrier, a complex output signal transforms into a regular train of pulses. However, its frequency remains unchanged.

Similar type of frequency transforming have been found for models of the Belousov-Zhabotinsky reaction [9,15] (the Rovinsky-Zhabotinsky and the Oregonator models). Moreover, simple frequency transforming modes have been observed in recent experiments with the Belousov-Zhabotinsky reaction, in which trains of excitable waves were crossing a passive region [22–24]. We expect that very complex modes of frequency transforming described in this paper will be also observed experimentally.

[1] *Oscillations and Travelling Waves in Chemical Systems*, edited by R. J. Field and M. Burger (Wiley, New York, 1985).

[2] See, e.g., J. Wiersig and Kang-Hun Ahn, Phys. Rev. Lett. **87**, 026803-1 (2001); M. Brons, P. Gross, and K. Bar-Eli, Int. J. Bifurcation Chaos Appl. Sci. Eng. **7**, 2621 (1997); T. Gilbert and R.W. Gammon, *ibid.* **10**, 155 (2001).

[3] M. Dolnik, I. Finkeova, I. Schreiber, and M. Marek, J. Phys. Chem. **93**, 2764 (1989).

[4] I. Finkeova, M. Dolnik, B. Hrudka, and M. Marek, J. Phys. Chem. **94**, 4110 (1990).

[5] M. Dolnik and M. Marek, J. Phys. Chem. **95**, 7267 (1991).

[6] M. Dolnik, M. Marek, and I.R. Epstein, J. Phys. Chem. **96**, 3218 (1992).

[7] A. Toth, V. Gaspar, and K. Showalter, J. Phys. Chem. **98**, 522 (1994).

[8] A. Lazar, Z. Noszticzius, H.-D. Försterling, and Z. Nagy-Ungvarai, Physica D **84**, 112 (1995).

[9] J. Sielewiesiuk and J. Górecki, J. Phys. Chem. A **106**, 4068 (2002).

[10] I.N. Motoike and K. Yoshikawa, Phys. Rev. E **59**, 5354 (1999).

[11] A.B. Rovinsky, J. Phys. Chem. **90**, 217 (1986).

[12] A.B. Rovinsky and A.M. Zhabotinsky, J. Phys. Chem. **88**, 6081 (1984).

[13] J. Sielewiesiuk and J. Górecki, J. Phys. Chem. A **105**, 8189 (2001).

[14] A. Zaikin and A.M. Zhabotinsky, Nature (London) **225**, 535 (1970).

[15] J. Sielewiesiuk and J. Górecki, Phys. Chem. Chem. Phys. **4**, 1326 (2002).

[16] R. FitzHugh, Biophys. J. **1**, 445 (1961).

[17] J. Nagumo, S. Arimoto, and S. Yoshizawa, Proc. IRE **50**, 2061 (1962).

[18] J. Sielewiesiuk and J. Górecki, Acta Phys. Pol. B **32**, 1589 (2001).

[19] B. Legawiec (private communication). See also B. Legawiec and D. Ziolkowski, Inzynieria chemiczna procesowa **2**, 293 (1988, in Polish).

[20] J. Farey, Philos. Mag. **47**, 385 (1816).

[21] J. Sielewiesiuk and J. Górecki, in *Proceedings of the 1st European Interdisciplinary School on Nonlinear Dynamics for System and Signal Analysis Euroattractor 2000, Warsaw, June 2000*, edited by Wlodzimierz Klonowski (Pabst Science Publishers, Lengerich, 2002).

[22] K. Suzuki, T. Yoshinobu, and H. Iwasaki, J. Phys. Chem. A **104**, 5154 (2000).

[23] J. Sielewiesiuk, PhD thesis, Institute of Physical Chemistry, Polish Academy of Science, Warsaw, 2002.

[24] Y. Igarashi, K. Yoshikawa, and J. Górecki, unpublished results of experiments performed with Ru-catalyzed Belousov-Zhabotinsky reaction at Physics Department, Kyoto University, Japan (2002).